Thermoelectric properties and devices of p-type $Bi_{0.4}Sb_{1.6}Se_{2.4}Te_{0.6}$ and n-type $Bi_2Se_{0.6}Te_{2.4}$ prepared by solid state microwave synthesis

Arej Kadhim Abbas, Arshad Hmood Abd Al Kadhim, Haslan Abu Hassan
Nano-Optoelectronic Research and Technology Laboratory (N.O.R.)
School of physics, Universiti Sains Malaysia
11800, Pulau Penang, Malaysia
Email: areejkadhim@yahoo.com

Abstract- This study reports on the fabrication of a chalcogen-based thermoelectric power generation (TEG) device using p-type $Bi_{0.4}Sb_{1.6}Se_{2.4}Te_{0.6}$ and n-type $Bi_2Se_{0.6}Te_{2.4}$ legs. Electrical power generation characteristics were monitored by changing both the temperature conditions and the number of p-n couples required to generate maximum power. The significance of the resistances, including the internal resistance (R_{in}) and contact resistance (R_c) between legs and electrodes, are discussed. The maximum open circuit voltage (V_{oc}) and output power (P_{max}) obtained with the 18 p-n couples device were 1480.5 mV and 273.2 mW, respectively, under the thermal condition of T_H=523 K hot-side temperature and ΔT = 184 K temperature difference.

I. INTRODUCTION

A thermoelectric power generation (TEG) device produces voltage between the hot and the cold sides when a temperature difference (ΔT) between the two sides is present as a result of thermoelectric effect (TE). TE includes Seebeck (S), Peltier, and Thomson effects. TE is also associated with other effects such as Joulean and Fourier effects [1].

The following are the advantages of these generators: no moving parts, small and lightweight, maintenance-free, acoustically silent and electrically "quiet," same-module heating and cooling, wide-ranging operating temperature, and environmentally friendly [2].

A practical TEG device generally consists of two or more elements of n-type- and p-type-doped semiconductor materials that are electrically connected in a series and thermally connected in parallel. The extra electrons in the n-material and the "holes" resulting from the deficiency of electrons in the p-material are the carriers that move heat energy through the TE material. Most TEG devices are fabricated using an equal number of n-type and p-type elements, where a pair of n and p elements forms a thermoelectric "couple" [3].

Yet, enhancing in the TE properties is strongly required for empirical applications. One approach to enhance the TE properties is optimization of the doping effective route. For example, recent devices use Bi_2Te_3, a semiconductor, which when alloyed with antimony (Sb) or selenium (Se) becomes an efficient TE material for refrigeration or for portable power generation [4]. As an alternate approach, researchers have attempted to improve the efficiency of materials based on Bi_2Te_3 by creating structures with one or more reduced dimensions [5]. In one case, an n-type Bi_2Te_3 has been shown to have improved S. However, S and electrical conductivity (σ) have a trade-off; a higher S results in decreased carrier concentrations and decreased σ [6].

In our study, we fabricated 9 and 18 couples of TEG devices using solid-state microwave synthesis. We focused on the properties of two TEG devices that use $Bi_{0.4}Sb_{1.6}Se_{2.4}Te_{0.6}$ as p-type and $Bi_2Se_{0.6}Te_{2.4}$ as n-type. Fundamental physical parameters of the p-type and the n-type samples, such as S, σ, and power factor (P_{factor}), were subsequently examined.

II. EXPREIMENTAL

Bi, Sb, Se, and Te that were used in this study were highly pure powders (99.999%). The typical element ratio for the preparation of p-type $Bi_{0.4}Sb_{1.6}Se_{2.4}Te_{0.6}$ is as follows: 0.3071g Bi, 0.7156g Sb, 0.6961g Se, and 0.2812g Te. The n-type $Bi_2Se_{0.6}Te_{2.4}$ was prepared by mixing 1.0834g Bi, 0.1228g Se, and 0.7938g Te. The p-type and n-type ingots were fabricated through a solid-state microwave synthesis that was described in a previous literature [7]. The samples were irradiated in an 800 W (100% power) MS2147C microwave oven (LG) at 2.45 GHz for 10 min. Bright, whitish-blue plasma was observed emerging from both the ampules from the first minute of microwave exposure. The temperature of the samples was measured using an OS524E infrared thermometer (OMEGA SCOPE) with values 898K for p-type sample, whereas 873K for n-type sample. Selected portions of the ingots were imaged using field emission scanning electron microscopy (FESEM) (Leo-Supra 50VP,Carl Zeiss, Germany).

After grinding, the samples were then characterized to determine their crystallization via X-ray diffraction (XRD, PANalytical X'Pert PRO MRD PW3040, Almelo, The Netherlands). The resultant powders were pressed into disk shapes (5 mm diameter and 3.5 mm thickness) through cold pressing at 10 tons. The Seebeck coefficient (S) was determined by the slope of the linear relationship between the thermoelectromotive force and the temperature difference between the two ends of each sample. The electrical conductivity (σ) was measured using the standard four-probe dc method under a vacuum of 10^{-3} mbar within temperatures ranging from room temperature to about 523 K.

The assembly of 9 and 18 couples from these pellets was placed between two alumina plates with the corresponding dimensions of 50 mm × 25 mm and 50 mm × 50 mm, respectively, which served as hot and cold ends for the relevant TE pellets. By using Ag paste and Cu plates, the Ag paste–Cu plates–Ag paste electrodes were made on the inner surface of the alumina substrate. The devices were then dried at room temperature for one day to metalize the electrodes on the devices. To evaluate device performance, the bottom alumina plate was heated up to 523 K by one brass block as heater for the device, and the top plate was cooled by another brass block with circulated cooling water. ΔT between the hot and the cold sides was measured by two digital K-type E© Sun (ECS820C) thermocouples near the inner surface of the alumina substrates. ΔT along the length of the devices was approximately equal to the difference in interface temperatures between the hot alumina plate T_H and the cold alumina plate T_C. The current-voltage (I-V) lines and the current-power (I-P) curves of power generation were performed in the air by sweeping the load resistance (R_L) using the variable resistance box. The open circuit voltage and many other voltages at the condition of power generation were measured by a voltage meter (Keithley 197).

III. Results and Discussion

A typical FESEM image of the surface morphology of the ingots $Bi_{0.4}Sb_{1.6}Se_{2.4}Te_{0.6}$ prepared through solid-state microwave synthesis is shown in Fig. 1(a). Hexagonal rods with polished surfaces and different widths and lengths were observed. The addition of Se to Bi_2Te_3 compound, the FESEM observations revealed the appearance of a typical layered and well-packed structure, which indicating that Se alloying is an effective approach for crystalline refinement, as shown in Fig. 1(b). XRD experiments were carried out to determine the structure of the powder samples, and the results are shown in Figs. 2. In Fig. 2(a) the XRD pattern of $Bi_2Se_{0.6}Te_{2.4}$ powder was showed. All the peaks in this pattern can be indexed according to JCPDS15-0863 and 33-0214 for Bi_2Te_3 and Bi_2Se_3, respectively, rhombohedral structure (R3m). In Fig. 2(b), all the XRD peaks of $Bi_{0.4}Sb_{1.6}Se_{2.4}Te_{0.6}$, which can be

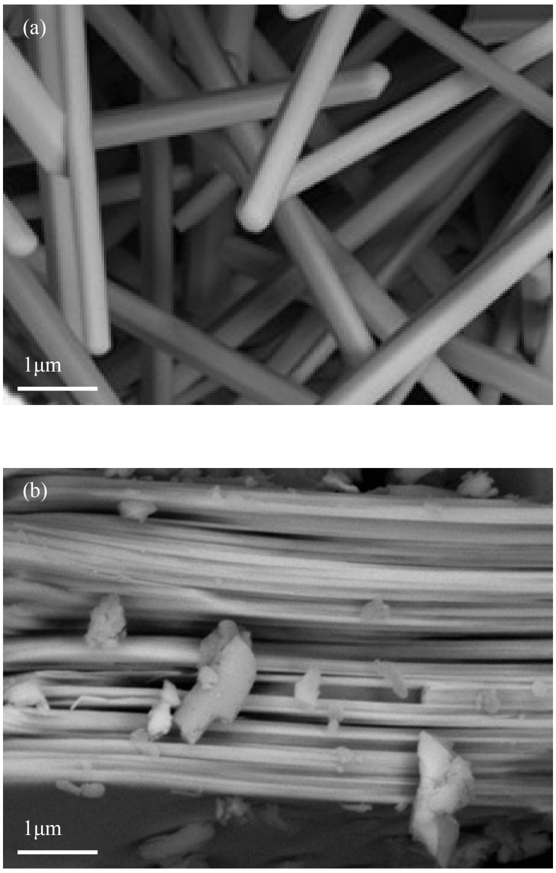

Fig. 1. Felid emission scanning electron microscopy image (FESEM) of (a) $Bi_{0.4}Sb_{1.6}Se_{2.4}Te_{0.6}$ and (b) of $Bi_2Se_{0.6}Te_{2.4}$ ingots.

indexed as the rhombohedral phase of Bi_2Te_3, Sb_2Te_3, and Bi_2Se_3 (JCPDS15-0863, 15-0874, and 33-0214, respectively) with a small amount of Sb_2Se_3 phase, appeared as (400), (331), (060), and (412). The diffraction peaks (015) displayed an apparent shift to a higher angle with increasing Se content, which is mainly due to the smaller atomic radius of Se (1.15 Å) compared with that of Te (1.4 Å).

The transport properties of p- and n-type samples in terms of σ, S, and P_{factor} were investigated from 300 to 523 K (Figs. 3 to 5). Both sample types had nearly the same behavior as σ, which gradually decreased as the experimental temperature increased, that is, a degenerate semiconductor (Fig. 3). σ for the p-type $Bi_{0.4}Sb_{1.6}Se_{2.4}Te_{0.6}$ sample (σ_p) varied from 4.96×10^5 S/m at 300 K to 1.79×10^5 S/m at 523 K, whereas σ for the n-type $Bi_2Se_{0.6}Te_3$ sample (σ_n) was from 1.99×10^4 S/m at 300 K to 1.74×10^4 S/m at 523 K. The behavior of the σ of the two types contrary to its S. S for both types of the samples gradually incr-

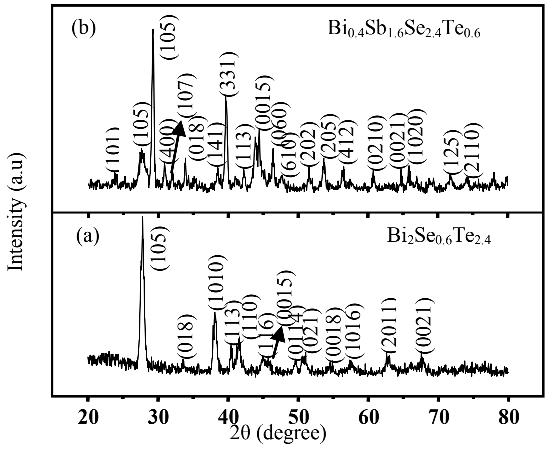

Fig. 2. X-ray diffraction of (a) $Bi_{0.4}Sb_{1.6}Se_{2.4}Te_{0.6}$ and (b) of $Bi_2Se_{0.6}Te_{2.4}$ powders.

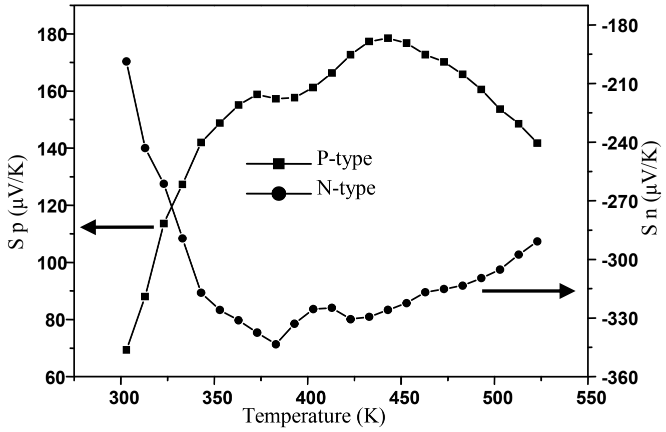

Fig. 4. Temperature dependence values of the Seebeck coefficient of p- and n-type samples.

ease as the temperature increases. As shown in Fig. 4, S of the p-type sample (S_p) was 178.5 at 443 K, and for n-type (S_n) was -330.6 μV/K at 423 K. σ and S were influenced by the incorporation of Se atoms into the crystal lattice, thus changing the formation energy of the lattice defects in the mixed crystals [4]. As evident in Fig. 5, the temperature behaviors of P_{factor} for the p-type and n-type samples were similar: increasing with increasing temperature, achieving a maximum, and then decreasing with further increases in temperature. It indicated that p- and n-type samples can be appropriately used at low temperatures. $P_{factor\text{-}P}$ values obtained for p-type samples were larger than those for n-type sample within the entire temperature range investigated. The maximum $P_{factor\text{-}P}$ measured was 7.47 mW/mK^2 at 373 K, as previously reported [7], whereas the maximum $P_{factor\text{-}n}$ was 2.22 mW/mK^2 at 383 K. The output voltage and the output power of the fabricated 9(D_1) and 18 (D_2) couples versus the current were measured by sweeping R_L at several temperature conditions, as shown in Figs. 6 and 7.The open-circuit voltage (V_{oc}) that is equal to the intercept of the I-V line reached 586 mV and 1480.5 mV for D1 and D2, respectively, at ΔT of 184 K and T_H of 523 K, which are in agreement with the expression $V=V_{oc}-R_LI$. It is lower than that calculated S–T curves of both p-and n-type legs ($V_{calculated} = (S_p-S_n) \times \Delta T \times n$, where n is the number of couples). This voltage loss could have originated from many factors including low thermal conductivity of alumina substrate and unfavorable junctions between the TE legs and the electrodes [8]. I-P curves illustrated in Figs. 6 and 7 exhibit the parabolic curves of the output power (P_{out}); an analysis to plots of I-V lines

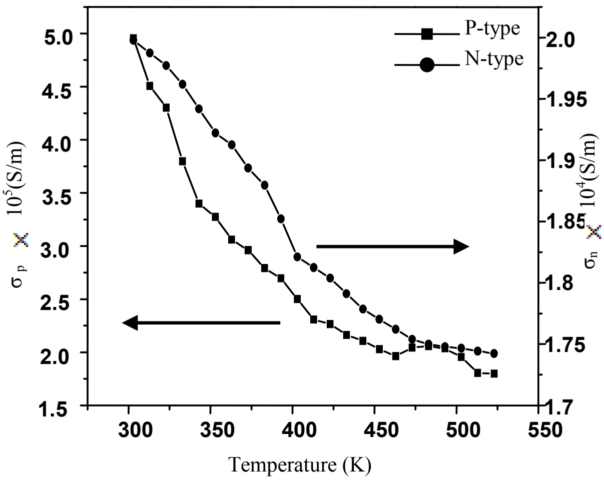

Fig. 3. Temperature dependence values of the electrical conductivity of p- and n-type samples.

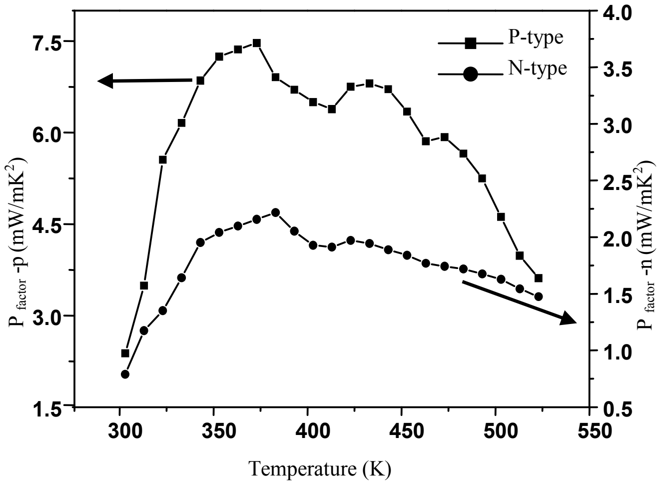

Fig. 5. Temperature dependence values of the power factor of p- and n-type samples.

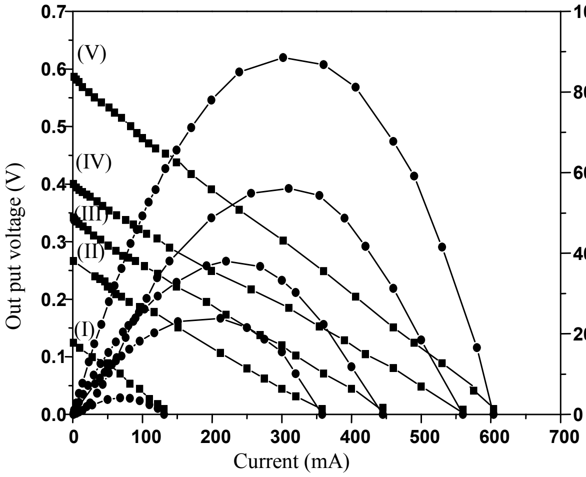

Fig. 6. The power generation characteristics of the TEG device that comprises 9, where (I)ΔT=27,(II)ΔT=66(III)ΔT=104(IV)ΔT= 145,and (V) ΔT=184K.

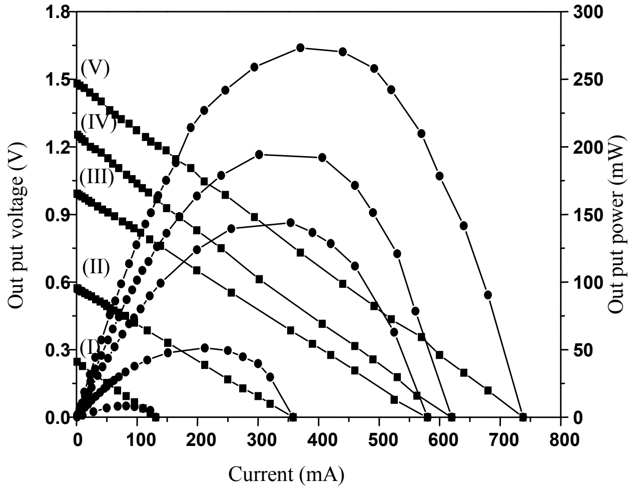

Fig. 7. The power generation characteristics of the TEG device that comprises 18, where (I)ΔT=27,(II)ΔT=66(III)ΔT=104(IV)ΔT= 145,and (V) ΔT=184K.

allows the observation of an increasing in the P_{out} with the ΔT. The explanation for this observation results from the rise of the ΔT, whose consequence is an increase in the output voltage(V_{out}).As high is this V_{out}, the high will be the output current (I_{out}) for a given R_L, and therefore will be the dissipated power in the external load. Considering several values for the R_L, it was also possible to obtain for the P_{out}, versus the I_{out} (or versus the R_L). The maximum output power (P_{max}) values were 88.5 and 273.2 mW for D1 and D2, respectively, at the thermal condition of 523 K T_H and ΔT = 184 K, which means these results could be comparable with the results of Wang et al. [4]. It was investigated that the powers of the devices improved by increasing the number of couples between the hot and the cold sides. Based on these results, V_{oc} and P_{max} systematically increased with the number of p-n couples, indicating that TE power could be simply controlled by a change in the module design.

The internal resistance (R_{in}) of each device corresponding to the slope of the I-V lines was directly obtained by the measured system. The ideal internal resistance (R_{id}) was calculated by the sum of the resistance values of p-type and n-type samples. With R_{in} and R_{id}, contact resistance (R_c) can be obtained by R_c=R_{in}-R_{id} [2]. The resistance values of D_2 (R_{in}=2Ω and R_c=1.57 Ω) were two times larger than those of D_1 (R_{in} =0.97 Ω and R_c=0.754 Ω), which could be attributed to the differences in size and electrode contact areas among elements [9]. These results demonstrate that, with the relationship between R_c and P_{max}, R_c should be minimized for each device because it plays a key role in TEG device performance. Two methods were adopted to optimize the device performance. First, the surface of the alumina plates was treated with NaOH solution to increase roughness and to enhance both mechanical strength and electrical contact between the alumina plates and the Cu electrodes. Second, the ends of p-type and n-type samples were grooved to increase the surface area, also improving the mechanical and the electrical properties of the contacts [2]. Electrical and thermal contacts are known to play an important key role in improving the device-manufacturing factor (MF). MF represents the cumulative influence of various parameters in the fabrication process on the quality of the devices, and it is defined as MF = R_{id}/R_{in} [8]. In the present research, MF at ΔT of 184 K reached 22.3% and 21.5% for D1 and D2, respectively, which could be attributed to the value of the Rc as previously mentioned. Based on the data obtained, the good TEG properties originally came from the relatively high electrical properties of p-type and n-type samples that were prepared by solid-state microwave synthesis.

IV. CONCLUSIONS

TE materials p-type $Bi_{0.4}Sb_{1.6}Se_{2.4}Te_{0.6}$ and n-type $Bi_2Se_{0.6}Te_{2.4}$ were prepared via solid-state microwave synthesis. TEG devices were fabricated and characterized in terms of high V_{oc} and P_{max}. A maximum V_{oc} and P_{max} of 1480.5 mV and 273.2 mW, respectively, were achieved in the device with 18 p-n couples with T_H of 523 K and ΔT of 184 K. V_{oc} and P_{max} increased with ΔT and also systematically increased with the number of p-n couples. Based on these results, the device using p-type $Bi_{0.4}Sb_{1.6}Se_{2.4}Te_{0.6}$ and n-type $Bi_2Se_{0.6}Te_{2.4}$ worked successfully and it was stable with satisfactory TE performances.

ACKNOWLEDGMENT

This work was supported by the (PRGS) 1001/PFIZIK/844091 of the Universiti Sains Malaysia (USM).

REFERENCES

[1] Y. Jiang, J. Zhou and X. Zhang, "Analytical model of parallel thermoelectric generator", Appl. Energy, vol. 88,pp. 5193–5199, 2011.

[2] L. Han, Y. Jiang, S. Li, H. Su, X. Lan, K. Qin et al., "High temperature thermoelectric properties and energy transfer devices of $Ca_3Co_{4-x}Ag_xO_9$ and $Ca_{1-y}SmyMn_{O3}$", J Alloys Compd. vol. 509, pp. 8970– 8977, 2011.

[3] A.G. Agwu Nnanna, W. Rutherford, W. Elomar, B. Sankowski," Assessment of thermoelectric module with nanofluid heat exchanger", Appl. Therm. Eng. vol. 29, pp.491–500, 2009.

[4] S. Wang, W. Xie, H. Li, X. Tang,"Enhanced performances of melt spun Bi2(Te,Se)3 for n-type thermoelectric legs", Intermetallics, vol. 19, pp.1024–1031.2011.

[5] J. Kang, J.-S. Noh and W. Lee," Simple two-step fabrication method of Bi_2Te_3 nanowires", Nanoscale Res. Lett., vol. 6, pp. 277–280, 2011.

[6] B.Y. Yoo, C.-K. Huang, J.R. Lim, J. Herman, M.A. Ryan, J.-P. Fleurial et al.," Electrochemically deposited thermoelectric n-type Bi_2Te_3 thin films", Electrochim. Act., vol. 50, pp. 4371–4377, 2005.

[7] A. Kadhim, A. Hmood, H. Abu Hassan," Novel hexagonal rods and characterization of $Bi_{0.4}Sb_{1.6}Se_{3x}Te_{3(1-x)}$ using solid-state microwave synthesis", Mater. Lett., vol. 81,pp.31–33, 2012.

[8] D. Zhao, C. Tian, S. Tang, Y. Liu, L. Jiang, L. Chen," FabricationofaCoSb3-based thermoelectricmodule", Mater. Sci. Semicond. Process., vol. 13, pp. 221–224, 2010.

[9] W. Shin, N. Murayama, K. Ikeda, S. Sago. Thermoelectric power generation using Li-doped NiO and (Br, Sr)PbO_3 module. J. Power Sour. 103 (2001) 80-85.